PROCEEDINGS, 48th Workshop on Geothermal Reservoir Engineering
Stanford University, Stanford, California, February 6-8, 2023
SGP-TR-224

Petrology and Hydrothermal Alteration Mineral Distribution of Wells LA-9d and LA-10d in Aluto Geothermal Field, Ethiopia

Dereje MOGES

P. O. Box:

deremogues@gmail.com

Keywords: Aluto geothermal field, Igneous rocks, Major oxides, tracer elements, XRF, XRD, Alteration minerals.

ABSTRACT

Lithology of the two wells was identified using the main oxides obtained using the XRF method. Twenty-four (24) cuttings with different degrees of alteration were analyzed to determine and identify the rock types, by plotting these well samples on special diagrams, and correlate with the regional rocks. The results for the analysis of themain oxides and trace elements of 24 samples are presented. Alteration analysis in the two well samples was conducted for 21 samples from two wells for identifying clay minerals. Bulk sample analysis indicated quartz, illite & micas, calcite, cristobalite, smectite, pyrite, epidote, alunite, chlorite, wairakite, diaspore and kaolin minerals present in both wells. Hydrothermal clay minerals such as illite, chlorite, smectite and kaoline minerals were identified in both wells by X-ray diffraction. High temperature hydrothermal minerals; such as, wairakite, biotite, and epidote exists in both wells based on the X-ray diffraction analysis result.

1. INTRODUCTION

The Aluto Volcanic Complex (AVC) geothermal prospect is located in the floor of the Main Ethiopian Rift (MER), close to its eastern escarpment, about 200 km south of Addis Ababa (Fig. 1). This prospect has beenan important target for geothermal development. Since 1969 a number of investigations were undertaken, and, in the 1980's, eight deep exploratory wells were drilled which resulted in the discovery of a geothermal field ofcommercial interest and in the installation of a small geothermal power plant. In view of the full development of the Aluto geothermal resources, it was planned to extend the detailed exploration beyond the sector now under development, with the final objective to increase the electric potential of the prospect from the present 35 MW new project to an additional 35 and possibly 70 MW. Recently drilled two wells, LA-9D and LA-10D, are part of this geothermal development activity. A geothermal system in this area is of liquid dominated on the basis of the results of discharge test performed at the two wells. Hydrothermal manifestations in the study area are hot springs (40 - 100°C), fumaroles (close to 100 °C), hot and warm ground associated with hydrothermal alteration.

The objective of this study is to perform laboratory analysis for chemical composition and minerals of cuttings from these two wells with XRF and XRD analyses, to classify igneous rocks and identify minerals as well as alteration minerals (Timothy, 1989). Finally, to estimate formation temperature of different rock units of the wells.

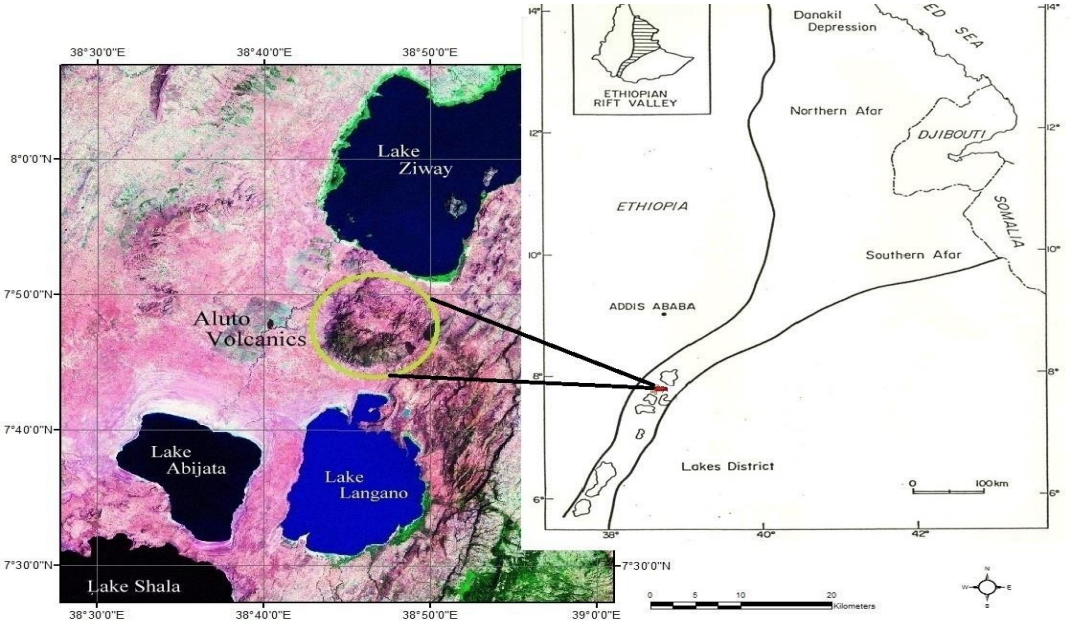

Figure 1. Location map of Aluto Volcanic Complex (WJEC, 2015).

2. GEOLOGICAL AND TECTONIC SETTING

Since the AVC is situated close to the eastern margin of the rift, its eastern portion directly overlies the rift floor volcanism that is younger than 2 Ma. Volcanism is down faulted towards the rift axis, hence the AVC itself is tilted to the west with more than 1000 m thick products, whereas at the eastern caldera margin thickness of AVC products does not exceed 300 m. Volcanic products related to the AVC cover an area of about 120 km^2 forming a rhombic area elongated in a NW-SE direction (Fig. 2).

The Ethiopian rift system being an active rift type, up-doming was followed by volcanism and rifting. The earliest episodes took place in the Southern Ethiopia Rift (SER) and the Afar Rifts, before 25 Ma (e.g., Davidson and Rex, 1980). Rift propagation proceeded both from the south and north directions towards the Main Ethiopian Rift (MER) (e.g. Bonnini et al., 2005). Rifting in the MER did not start until about 8 Ma (Abebe et al., 2010), possibly due to the presence of transversal structures, that stopped propagation of rifting for a long geological period, and it can be shown the general local trend of three faults in Aluto having a NE- SW similar with the regional fault trend Wonji Fault Belt (WFB) (Fig. 2).

Lithologies younger than 1.6 Ma are related to the NE-SW trending fracture systems together with their transversal structures that are NW-SE and ENE-WSW oriented. After 1.6 Ma drifting direction of the Somalian plate changed from SE towards nearly E (Boccaletti et al.,1999, Bonnini et al., 2005, Corti, 2008, 2009), causing the development of N-S/NNE-SSW trending fracture systems known as the Wonji Fault Belt (WFB). The AVC, being a Late Pleistocene to Holocene structure, is governed by the WFB, although the transversal structures (NW-SE and ENE-WSW) also played important roles.

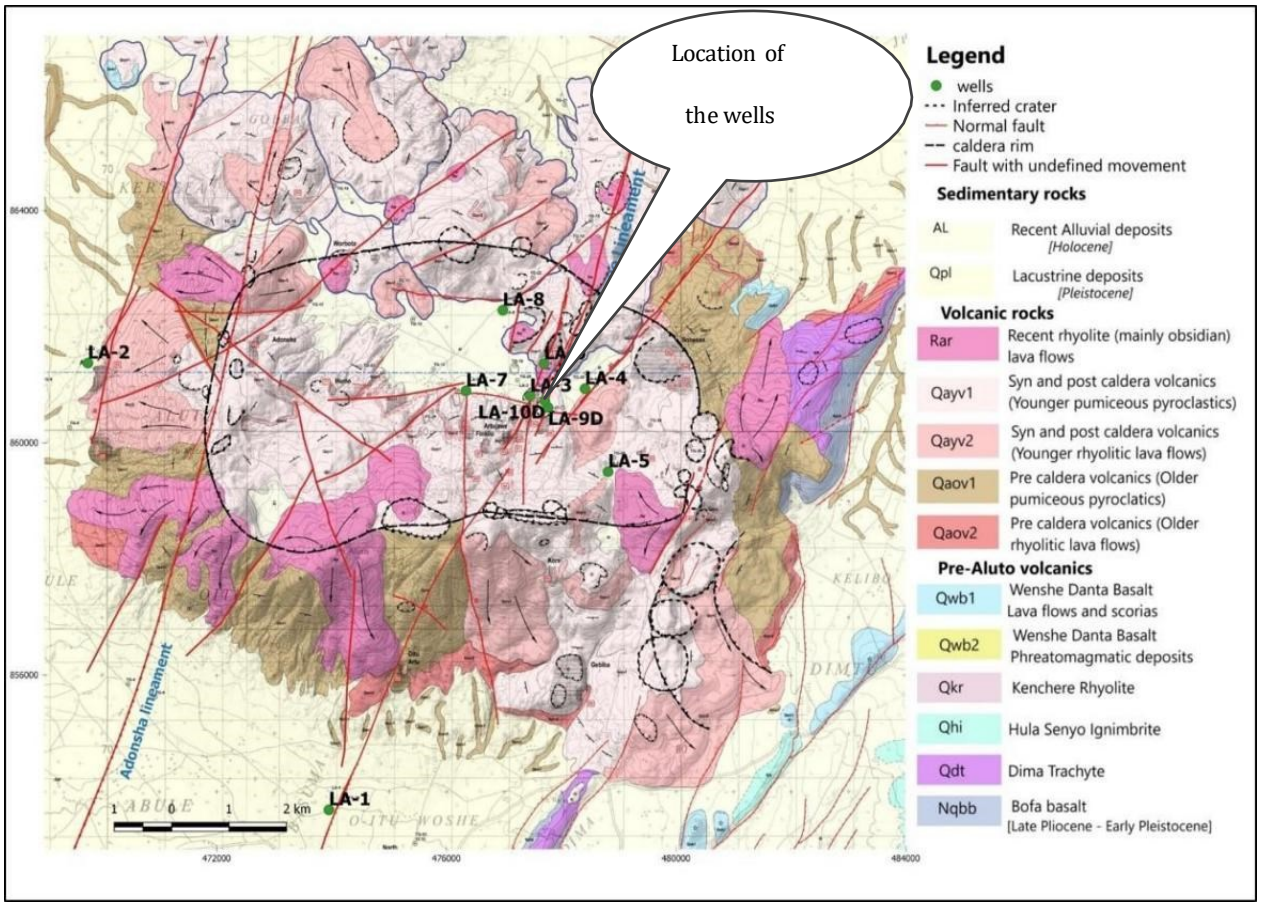

Figure 2. Location map of Wells LA-9D and LA-10D in Aluto (ELC, 2014).

3. METHODOLOGY

3.1. Materials and Methods

Drilling cuttings from Wells LA-9D and LA-10D were used for analysis. The depth of Well LA-9D is 1920m and about 384 cutting samples were recorded on site. The depth of Well LA-10D is 1952m and around 390 cutting samples were recorded on site, but the quantity of the cuttings is less compared to that of Well LA-9D because of total loss of circulation at some sections. For XRD analysis 21 samples were selected from the two wells based on degree of alteration, and 24 samples for XRF analysis.

The first approach was sample preparation for analysis; hence the samples used for analysis of the chemical composition and petro logical investigation with XRF spectrometer should have its own criteria of grain size and moisture content. For this purpose, different sample preparation techniques were adopted with instruments shown in Fig.3. Firstly, 1) drill cuttings were dried for 24 hrs. in oven with 45˚C and

100°C high cut, then crushed to a powder using a miller for 15 min. Sample holder was washed with ethanol to remove water between each milling process, 2) Pellet was prepared for each 24 samples with a presser with 3-4t load pressure for 30 sec and 20t pressure for 2 min with a careful handling of each sample in order to prevent contamination. Water and ethanol were used for cleaning, 3) For loss on ignition (L-O-I) measurement, 1gm of each sample was heated in the oven for 90 min at 120°C high cut at 105°C and weighed, then inserted in the electronic furnace adjusting the temperature to 1000°C at maximum until it reached 200°C for about 4 hr, and finallyweighed after it was cooled for 10-15 min in a desiccator. Based on the recorded results, L-O-I was calculated with the help of Excel data sheet for final measurement of each samples chemical composition and petrology with Rigaku Rix 3100 XRF.

Ultrasonic shaker

Centrifugal to precipitate clay

Pellet preparation with Presser

Samples set in Electronic Furnace

Rigaku Ultimate Iv X-Ray Diffractometer

X-ray Fluorescence

Figure 3. Sample Preparation Instruments and Analysis Equipment.

The results of the XRF analysis are plotted on a TAS (Cox et al., 1979) diagram in Figs. 4 and 5, in which, SiO_2 is on the horizontal axis and Na2O + K2O on the vertical axis. It can be observed that the samples are generally intermediate to acidic and some to mafic which

vary from sub-alkaline to calc-alkaline, which is a general trend. Based on the diagram, these rocks are in six ranges of basalt, basaltic andesite, trachy-andesite, andesite, dacite and rhyolite, which is in accordance with microscopic observations performed during on site drilling progress (WJEC, 2015). It seems that magmatic origin of these rocks is basaltic and basaltic-andesitic, and other trachy-andesite, dacitic and rhyolite rocks were created by differentiation and digestion of walls fromandesitic magma.

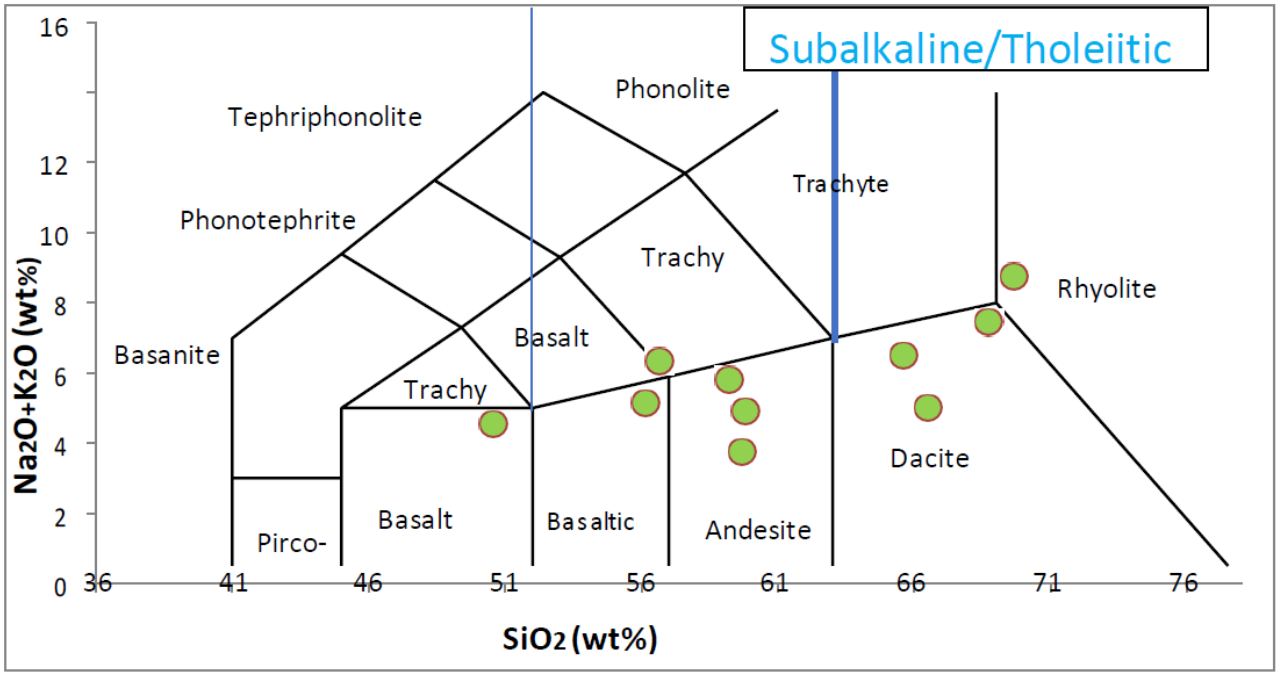

Figure 4. LA-9D well samples on TAS diagram.

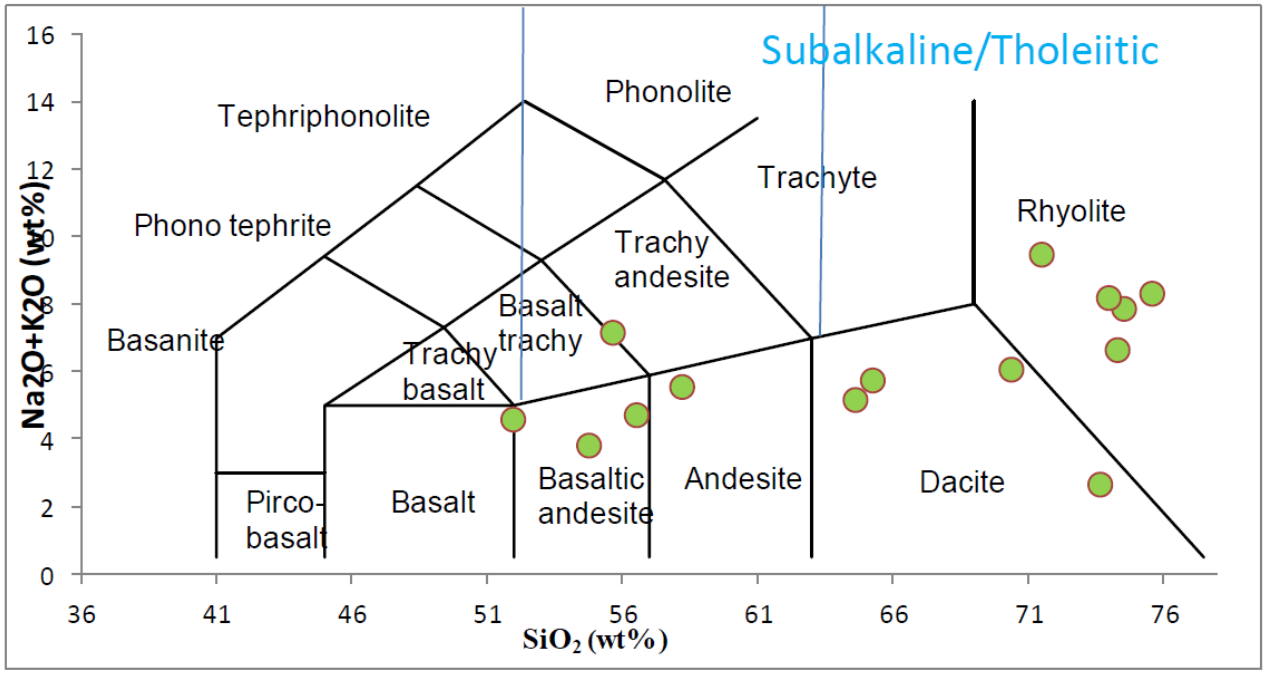

Figure 5. LA-10D well samples on TAS diagram.

3.2. Geochemistry

Weight percentage of main oxides were plotted against SiO_2 in Fig.6 for Well LA-9D and Fig.7 for LA-10D. Thef following results were obtained.

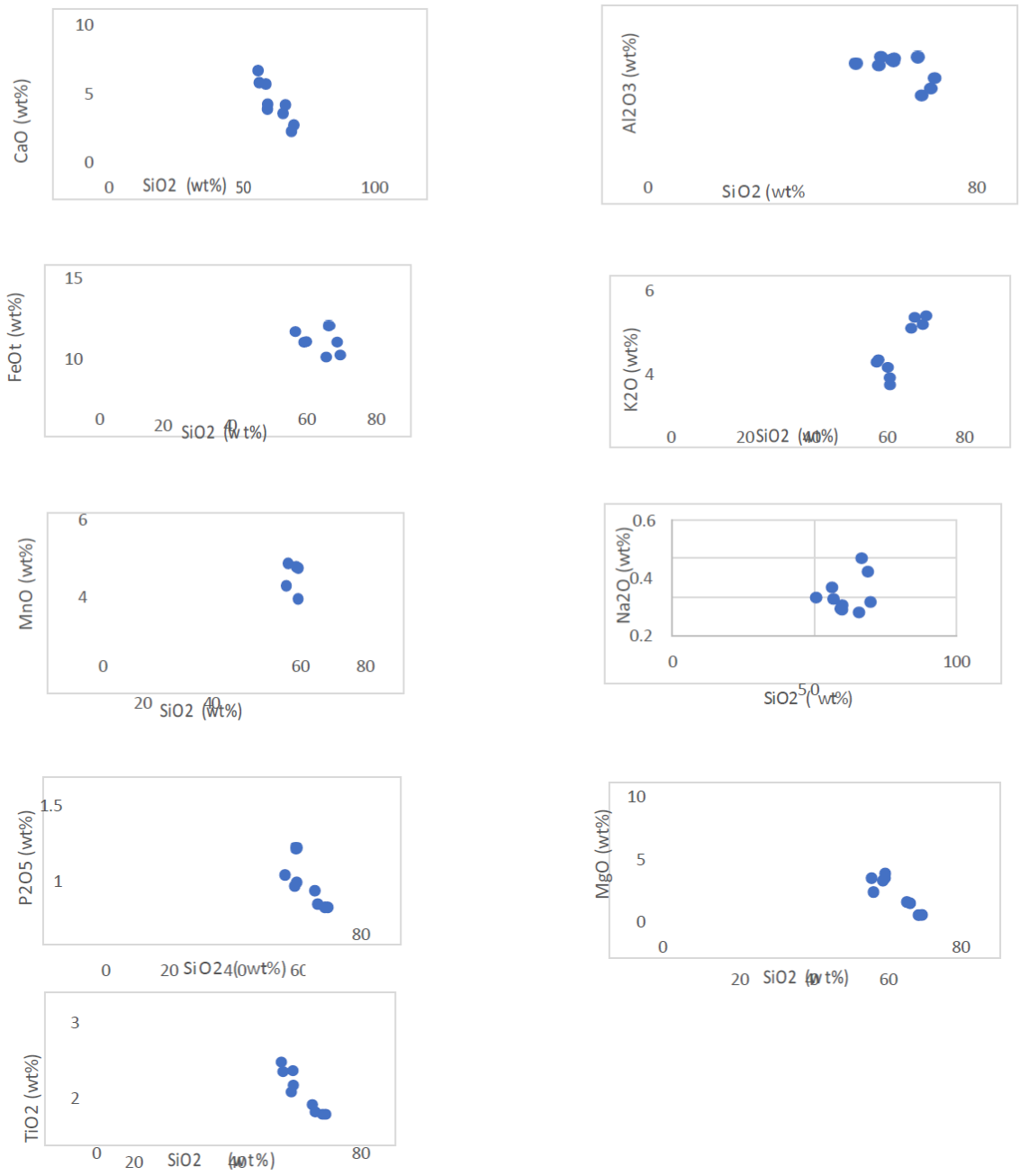

Figure 6. SiO_2 vs major oxides on Harker diagram for well LA-9D.

Na_2O with a relative decrease with an increase of SiO_2. In general, Na decreases with an increase of SiO_2 forthese six types of rocks. But more specifically, with an increase of SiO_2, Na also increases with a gentle slope in each type of rocks.

K_2O can also be observed in six rock types of this diagram. This diagram demonstrates that all rock types ofthis well show a significant change in the amount of K_2O against the increase of SiO_2 with a gentle slope.

CaO decreases with an increase of SiO_2 with a steep slope.

MgO shows a similar decrease slope of CaO with respect to the increase of SiO_2.

Moges

Al_2O_3 shows an overall decrease, which means aluminum decreases with an increase of SiO_2. With a more careful examination, it is evident that increase exists in all the separate types of rocks for this well samples. Andesitic rocks demonstrate positive gentle slope and dacite rocks demonstrate a positive steep slope.

TiO_2 negatively decreases steeply with an increase of SiO_2.

MnO shows also a relative decrease with an increase of SiO_2.

P_2O_5 content remarkably shows a steep slope of decreasing with respect to SiO_2 increase.

FeOt also decreases with an increase of SiO_2.

Most major oxides show an overall decrease with an increase of SiO_2 with gentle or steep slope. But there isalso the same trend of increase of K_2O with SiO_2 content increase.

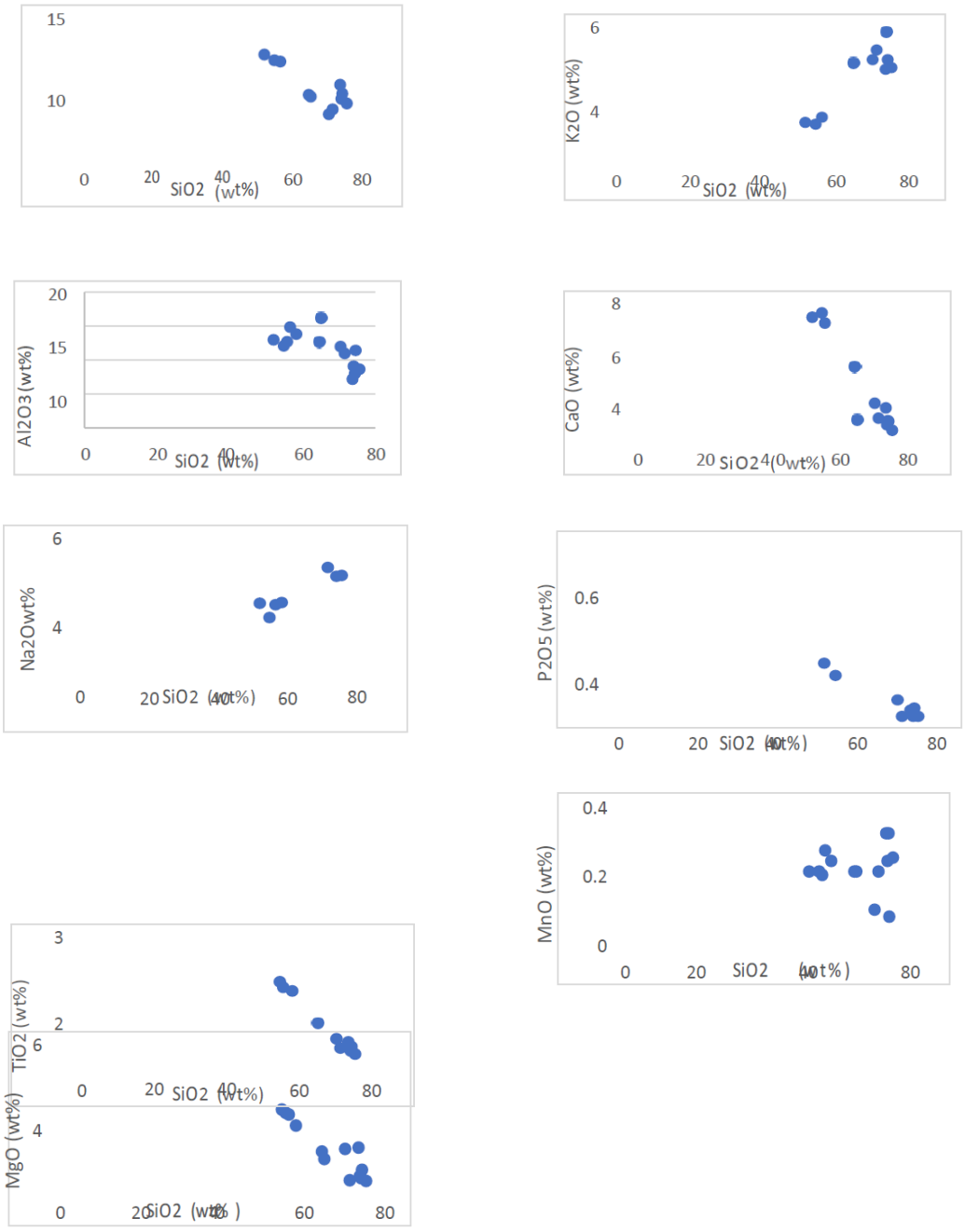

Figure 7. SiO2 vs major oxides on Harker diagram for well LA-10D.

For Well LA-10D, the results are summarized as follows:

Na_2O shows a relative decrease with increase of SiO_2, which is similar with LA-9D.

K_2O also shows a similar trend as LA-9D. It is clear that composition of K_2O is dominant compared to Na_2O in rhyolite, which is a general trend of igneous rocks.

CaO decreases with an increase of SiO_2 with a steep slope as LA-9D.

MgO shows the same decrease slope of CaO with respect to an increase of SiO_2.

Al_2O_3 shows an overall decrease with an increase of SiO_2. This means aluminum decreases with an increase of SiO_2. With a more careful examination, it is evident that increase exists in all the separate types of rocks for this well samples. Andesitic rocks demonstrate positive gentle slope and dacite rocks demonstrate a positive steep slope.

TiO_2 negatively decreases with an increase of SiO_2, and has a steep slope.

MnO shows also a relative decrease with an increase of SiO_2.

P_2O_5 also shows the same trend of decrease as LA-9D with a steep slope with respect an increase of SiO_2.

FeOt decreases with an increase of SiO_2.

It can be concluded that even though the changing trends for main oxides of igneous rocks are somewhat linear and it actually shows magmatic differentiation in these rocks, factors such as alteration (especially those samples with loss of ignition, which exceed 3% by weight), and magmatic contamination affected this trend (Table 1 & 2). The decrease or negative slope of major oxides indicates that there might have occurred a new magma addition with high silica content during fractional crystallization (i.e., wherein early-formed crystals are removed from the magma by crystal settling, leaving behind a liquid of slightly different composition), or magmatic differentiation.

Figure 8. Trace elements vs silica, and ratio of trace element with FeOt/MgO ratio.

Rb/Sr vs FeOt/MgO plot in Fig.8 shows relatively the same trend, one increases with the increase of the other for the two wells. Also, the same trend is observed in the Zr vs SiO_2 plot in Fig.9.

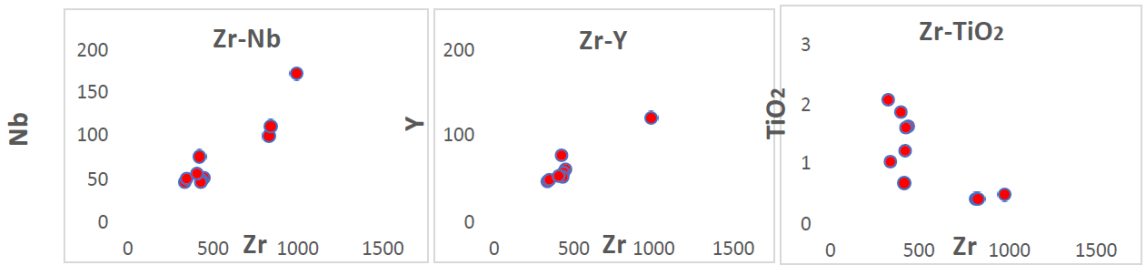

Figure 9. Trace elements vs Zirconium, and TiO_2 vs Zr for LA-9D.

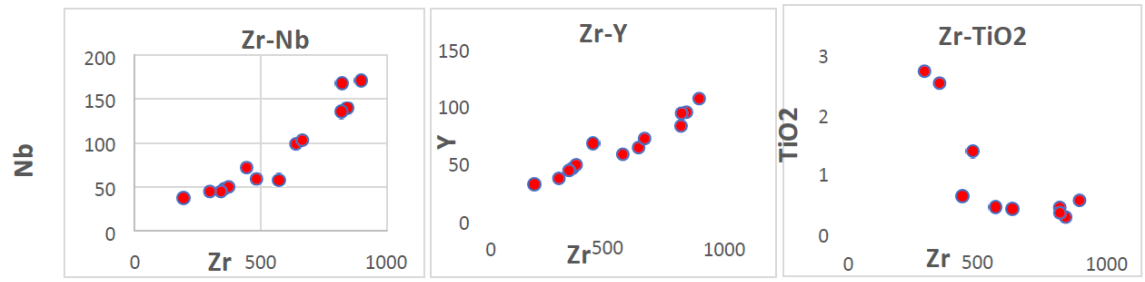

Figure 10. Trace elements vs Zr, and TiO_2 vs zircon for LA-10D.

Figures 9 and 10 present relationships between Zr and other trace elements. As we can see in both diagrams, there is a similar trend of change in the content of Nb, Y with that of Zr. On the other hand, an opposite trend for Zr-TiO_2. is observed.

3.3. Geochemistry based on type of magma

As was observed in Figs.4 and 5, rocks of the wells are in the range of sub-alkaline and tholeiitic. Figure 13 presents a plot of AFM diagram for (Na_2O+K_2O)-FeOt-MgO. From this figure, we can say that most of the samples are in the range of calc-alkaline series and some tend to be tholeiitic series.

Figure 11 shows a relationship for SiO_2-K_2O of Well LA-9D (Peccerillo & Taylor, 1976) diagram divides the magmatic series of well LA-9D samples into three series. Basaltic rocks and basaltic -andesitic rocks are high calc-alkaline, andesite rocks in calc-alkaline, and dacite and rhyolite rocks in to high calc-alkaline series (Fig. 11).

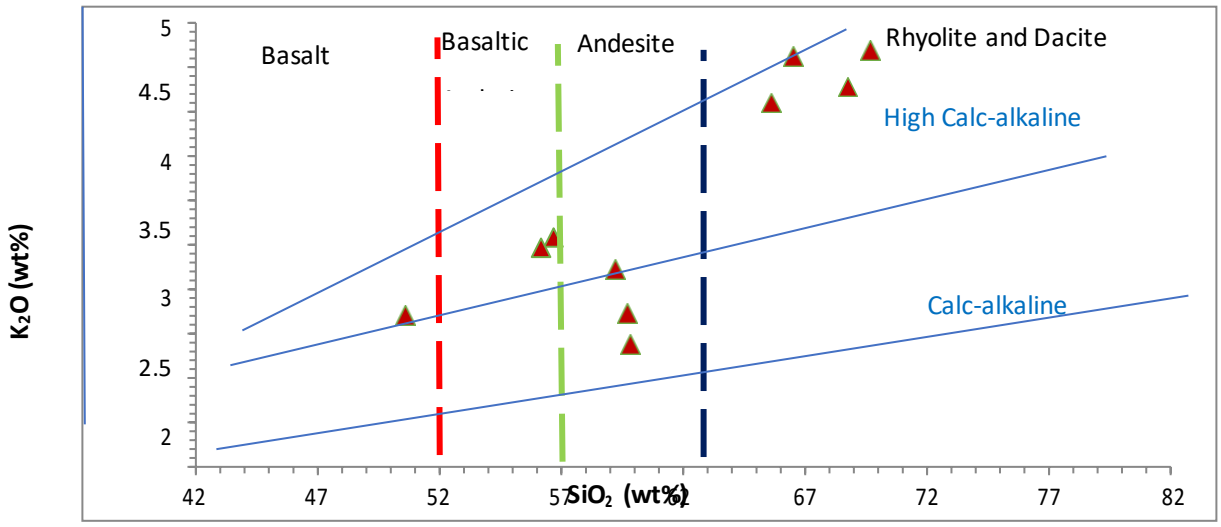

Figure 11. Well LA-9D samples on SiO_2-K_2O (Peccerillo and Taylor, 1976) diagram.

SiO_2-K_2O (Peccerillo and Taylor 1976) diagram divides the magmatic series of well LA-10D samples into the following series, basaltic-andesitic rocks are high calc-alkaline and medium calc-alkaline, andesitic rocks in high calc-alkaline, dacite and rhyolite rocks in high-medium calc-alkaline (Figure 12).

After plotting the data on Miyashiro (1974) diagram for SiO_2 and FeOt/MgO, it is observed that five of the LA-9D well samples are in the range of calc-alkaline series and five of the samples are tholeiitic. But almost samples of well LA-10D are tholeiitic, except a few of them observed to be calc-alkaline (Figures 14 and 15).

Most samples of the two wells are grouped under peraluminous rocks which means that it can be expressed chemically on a molecular basis as: $Al_2O_3>(CaO+Na_2O+K_2O)$.

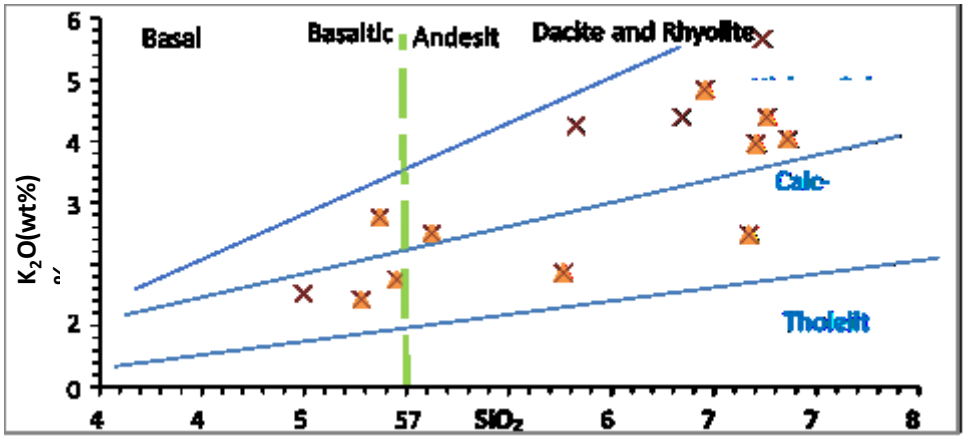

Figure 12. Well LA-10D samples on SiO2-K2O (Peccerillo and Taylor 1976) diagram.

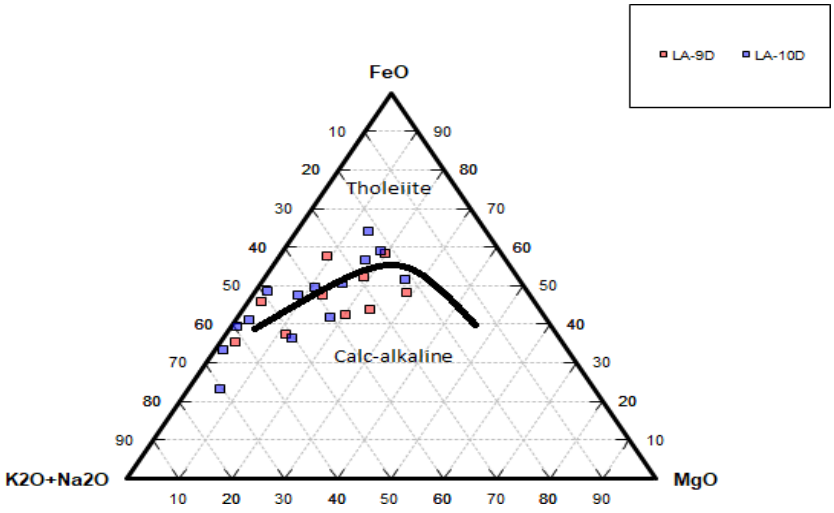

Figure 13. Plots of AFM [(Na2O+K2O)-FeO-MgO] ternary diagram for the well samples of LA-9D and LA-10D.

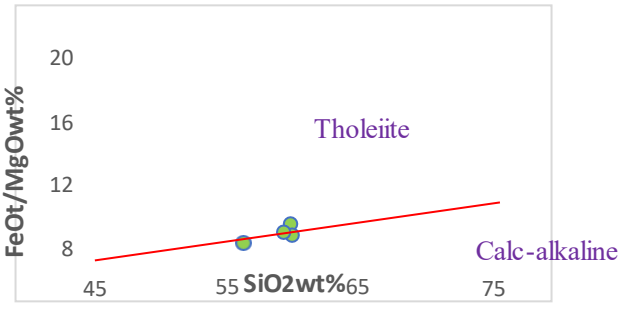

Figure 14. Miyashiro diagram of LA-9D.

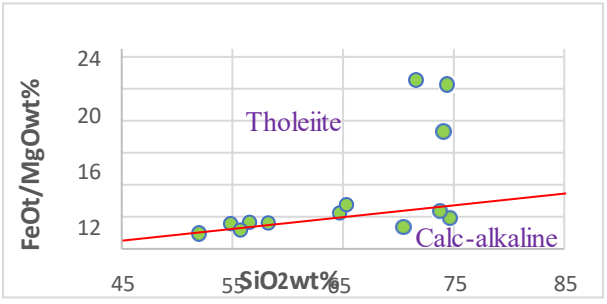

Figure 15. Miyashiro diagram of LA-10D.

Table 1. Results of the analysis of main oxides (wt.%) for the retrieved petrological samples of the wells.

No.	Sample No.	SiO_2	TiO_2	Al_2O_3	FeOt	MnO	MgO	CaO	Na_2O	K_2O	P_2O_5	L.O.I	Total
1	LA9(200)	69.665	0.371	11.525	5.037	0.174	0.436	2.637	4.051	4.696	0.000	1.22	98.592
2	LA9(405)	68.751	0.368	10.081	6.637	0.332	0.405	2.182	3.157	4.279	0.000	3.60	96.192
3	LA9(600)	66.52	0.44	9.13	8.65	0.40	1.36	4.10	0.38	4.62	0.04	3.93	95.640
4	LA9(800)	59.21	0.99	14.10	6.62	0.14	3.15	5.61	3.58	2.22	0.27	3.99	95.890
5	LA9(900)	59.713	1.585	13.836	9.909	0.134	3.354	3.796	2.014	1.728	0.748	2.95	96.817
6	LA9(1080)	65.62	0.64	14.44	4.76	0.12	1.46	3.43	2.39	4.10	0.21	2.62	97.170
7	LA9(1270)	56.673	1.560	14.463	7.945	0.189	2.234	5.727	3.746	2.584	1.256	3.15	96.377
8	LA9(1520)	50.582	2.028	13.540	9.554	0.197	5.754	8.773	2.831	1.703	0.415	4.43	95.377
9	LA9(1640)	59.827	1.178	14.274	6.702	0.157	3.717	4.153	3.514	1.383	0.315	4.48	95.220
10	LA9(1800)	56.16	1.82	13.29	9.32	0.25	3.34	6.53	2.65	2.47	0.41	3.44	96.240
11	LA10(440)	71.57	0.40	10.96	4.85	0.21	0.23	0.95	4.61	4.84	0.01	1.23	98.630
12	LA10(500)	74.60	0.43	11.40	2.59	0.08	0.67	0.76	3.46	4.39	0.05	1.29	98.430
13	LA10(580)	73.73	0.54	7.17	7.57	0.32	1.61	1.57	0.16	2.48	0.04	4.46	95.190
14	LA10(740)	54.81	1.93	12..06	10.23	0.21	3.22	7.34	2.40	1.43	0.21	5.99	93.840
15	LA10(840)	56.54	2.50	14.83	10.10	0.27	3.01	3.59	2.97	1.75	0.39	3.91	95.950
16	LA10(880)	75.62	0.26	8.63	5.52	0.25	0.19	0.21	4.27	4.03	0.01	0.77	98.990
17	LA10(1160)	74.06	0.42	9.05	6.02	0.24	0.41	0.55	4.22	3.96	0.03	0.84	98.960
18	LA10(1250)	64.68	1.36	12.58	6.45	0.21	1.44	4.04	3.29	1.86	0.24	3.64	96.150
19	LA10(1360)	58.25	1.72	13.80	8.32	0.24	2.54	4.67	3.06	2.50	0.54	4.13	95.640
20	LA10(1520)	55.71	1.80	12.67	7.34	0.20	3.08	6.72	4.37	2.76	0.51	4.50	95.160
21	LA10(1600)	51.97	2.70	12.96	10.87	0.21	5.64	7.07	3.03	1.52	0.27	3.54	96.240
22	LA10(1880)	70.44	0.61	11.97	4.33	0.10	1.56	1.85	1.63	4.39	0.09	2.82	96.970
23	LA10(1910)	65.29	0.97	16.19	6.27	0.21	1.13	0.83	1.50	4.25	0.07	3.09	96.710
24	LA10(1920)	74.37	0.33	7.98	6.59	0.40	0.32	0.78	0.98	5.66	0.01	2.38	97.420

Table 2. Results of the analysis of trace elements (ppm) for the retrieved petro logical samples of the wells.

Sample Name	SiO_2 (wt.%)	S	V	Cr	Co	Ni	Cu	Zn	Pb	As	Mo	Rb	Sr	Ba	Y	Zr	Ta	Nb
LA9(200)	69.7	0.0266	1	0	26	7	0	0.0178	0.001	0	20	104	14	235	84	831	0	97
LA9(405)	68.8	0.0383	9	19	0	22	19	0.0206	0	17	17	87	13	282	93	841	0	108
LA9(600)	59.7	0.2083	16	31	0	24	5	318	11	181	27	195	76	136	118	989	Nd	169
LA9(800)	56.7	0.0026	40	0	0	2	5	109	0	36	8	59	255	366	46	346	Nd	47
LA9(900)	50.6	0.0738	116	0	14	1	0.0016	0.0149	0	3	16	43	346	324	58	447	0	48
LA9(1080)	59.8	0.0067	20	0	1	7	5	156	7	30	11	99	286	403	74	422	Nd	73
LA9(1270)	66.5	0.3002	63	0	33	3	0.0001	0.0122	0.0011	0	11	56	483	402	54	434	0	45
LA9(1520)	59.2	0.0373	164	9	35	8	0.0004	0.0108	0.0003	0	7	36	460	306	44	333	0	43
LA9(1640)	65.6	0.1632	56	0	3	5	0.0001	0.0103	0.0004	2	21	29	390	231	49	429	0	43
LA9(1800)	56.2	0.0728	79	12	1	11	14	162	0	35	10	66	540	392	50	405	Nd	53
LA10(440)	71.6	0.0015	0	0	0	14	2	199	0	32	15	103	12	308	63	640	Nd	99
LA10(500)	74.6	0.1028	0	0	3	10	3	103	0	23	20	93	93	362	57	572	Nd	58
LA10(580)	73.7	0.1604	11	0	0	17	9	300	18	60	23	174	52	73	106	898	Nd	171
LA10(740)	54.8	0.0577	136	5	3	31	34	129	0	29	1	40	322	187	31	194	Nd	37
LA10(840)	56.5	0.0002	113	0	5	9	19	151	0	21	4	50	385	281	45	356	Nd	48
LA10(880)	75.6	0.0976	0	0	2	10	4	300	8	33	23	92	11	90	94	844	Nd	139
LA10(1160)	74.1	0.0277	2	0	4	8	20	292	2	31	23	90	36	94	82	821	Nd	135
LA10(1250)	64.7	0.01	36	0	0	5	17	167	7	32	12	42	542	644	49	484	Nd	59
LA10(1360)	58.3	0.0346	40	0	6	2	6	167	0	30	7	53	662	533	48	372	Nd	50
LA10(1520)	55.7	0.1683	63	0	2	0	10	119	0	29	9	85	464	475	43	342	Nd	45
LA10(1600)	52	0.0923	163	0	0	7	12	147	0	20	5	38	480	219	36	298	Nd	45
LA10(1880)	70.4	0.0371	17	3	0	11	10	156	16	37	12	119	223	487	67	444	Nd	72
LA10(1910)	65.3	0.0179	29	0	2	25	11	191	21	39	15	127	119	441	71	665	Nd	103
LA10(1920)	74.4	0.0236	0	0	0	9	12	253	15	39	17	211	45	88	93	823	Nd	168

4. XRD ANALYSIS

4.1. Materials and Method

In the laboratory, two types of powdered samples, namely bulk and oriented samples were prepared for X-ray diffraction (XRD) analysis. For bulk samples, at first, samples were crumpled in to smaller pieces and dried in an oven at 100˚C high cut and 45˚C for 24 hrs. to remove moisture. Then sample were crushed further to clay size with mortar and pestle. Finally, powdered specimen compressed on metal plate (pallet) as thin film inorder that XRD can analyze properly to determine alteration minerals (Hayashi, 1973; Hayashi, 2013).

In order to identify clay minerals from the drill cutting, oriented samples were prepared. At first samples were crushed into sand-gravel size. And immersed in to de- ionized water in beakers up to 200ml, after stirring it with spoon, it was put in an ultrasonic shaker (Fig. 3) for 15 min in order to dispense and suspended clay minerals in the solution. Then left for about 4 hrs. to let the clay suspended on the top and other heavy materials to sink at the bottom. The suspended clay solution at the top was transferred to another smaller beakers to let the samples stay centrifuged (Fig. 3) for 20 min. Then solute began to precipitate according to their specific density. Finally clay minerals appeared at the bottom and side of the smaller beakers. The collected clay minerals were dropped on a slide glass blade and air dried for 24 hrs. before XRD analysis. In order to separate different minerals with the same d-value in oriented analysis result, further EG (Ethylene Glycol) and HCl treatment was conducted.

4.2. Result and Discussion

Hydrothermal alteration minerals were identified in both wells such as, quartz, illite & micas, calcite, cristobalite, smectite, pyrite, epidote, alunite, chlorite, diaspore, montmorillonite, pyrophyllite, apophyllite and kaoline. The details of specific hydrothermal alteration minerals identified in each drill cuttings are summarized in Table 3. There is a wide range of clay minerals and other hydrothermal alteration minerals withdifferent thermal and chemical properties in each well (Reyes, 1990: Taguchi, 2001:Taguchi et al., 2003).

Table 3. XRD analysis of Well LA-9D and LA-10D samples.

	Minerals																	
Sample No.	Epidote	Quartz	Cristobalite	Alunite	Kaoline	Pyrophyllite	Smectite	Illite	Chlorite	Pyrite	Calcite	Plagioclase	Lizardite	Antigorite	Palygorskite	Sepiolite	Na-Mont.	Apophyllite
LA9(200)		X	X	X		X		X										
LA9(405)		X	X					X			X	X					X	X
LA9(600)	X	X			X		X	X		X	X					X		
LA9(800)		X		X	X		X	X		X	X	X	X	X	X	X	X	X
LA9(900)		X	X					X	X	X	X		X		X	X		X
LA9(1080)		X			X		X	X	X		X	X	X		X	X		X
LA9(1270)		X		X	X		X	X	X	X		X			X	X		X
LA9(1520)		X	X	X	X			X	X	X		X		X	X		X	
LA9(1640)		X	X	X	X			X	X				X	X	X	X	X	X
LA9(1800)		X	X						X		X	X		X	X	X		
LA9(1920)		X	X	X		X		X	X		X	X		X		X	X	X
LA10(420)		X		X			X	X			X	X			X		X	
LA10(600)		X		X			X	X	X		X		X			X		
LA10(760)		X	X					X	X			X	X	X		X		
LA10(895)		X	X			X		X	X	X		X				X		
LA10(1260)		X						X	X			X		X		X		
LA10(1340)			X		X			X	X	X			X	X	X	X		
LA10(1500)		X	X		X			X	X			X		X	X	X		
LA10(1620)		X						X	X	X		X		X	X			
LA10(1850)		X		X				X	X			X				X		
LA10(1930)		X	X	X				X	X						X	X		

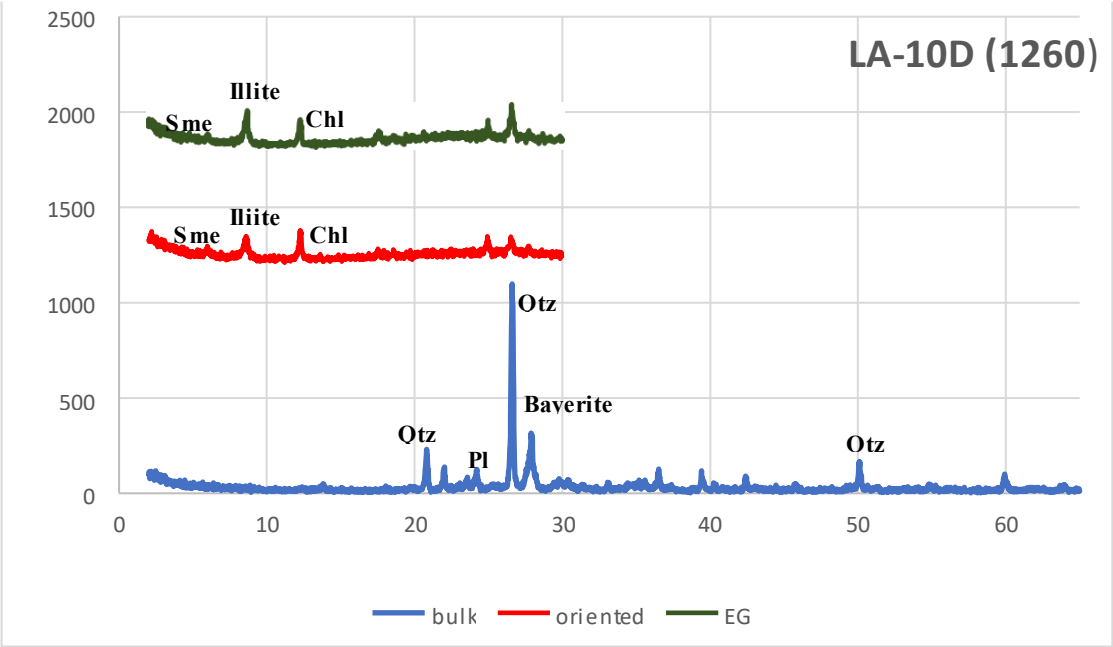

Figure 16. XRD pattern of bulk samples and oriented samples (Air-dry and EG)

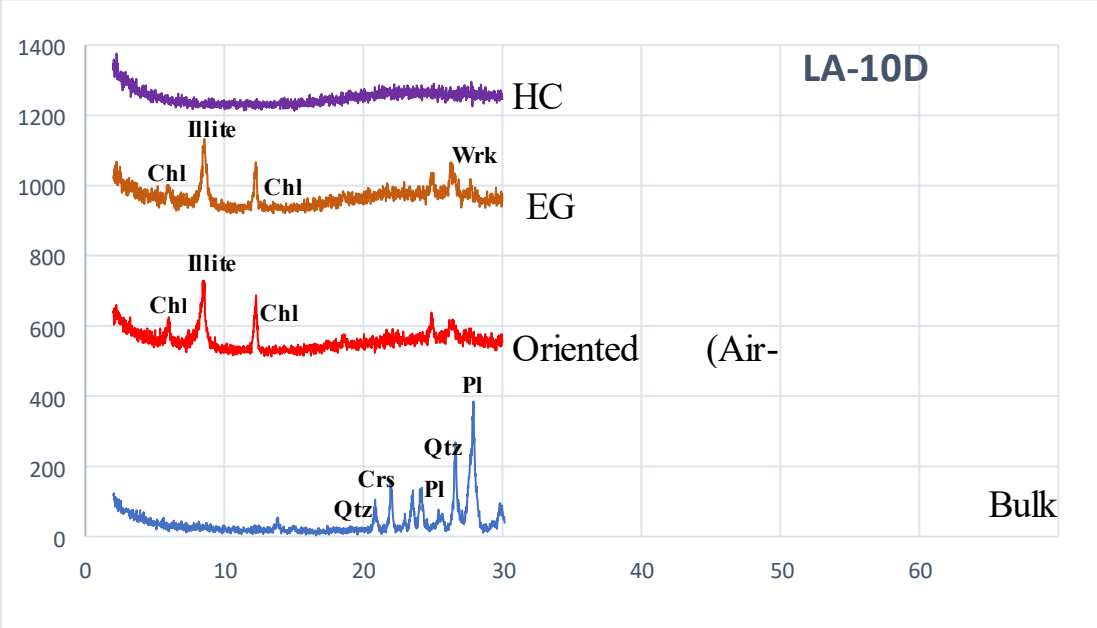

Figure 17. XRD pattern of bulk samples and oriented samples (Air-dry, EG and HCL).

5. CONCLUSION

Results of XRF analysis for the drilling cutting of Wells LA-9D and LA-10D present that they are generally classified as intermediate to acidic and some to mafic varying from sub-alkaline to calc-alkaline, which is a general trend. Based on the different diagrams applied in interpretation for classification of the samples rock types, they are in the range of basalt, basaltic-andesite, trachyandesite, andesite, dacite and rhyolite, which is in accordance with microscopic observations performed during drilling (WJEC, 2015). The magmatic origin of these rocks was basaltic and basaltic-andesitic. Other trachyandesite, dacitic and rhyolite rocks were formed by other processes such as

differentiation and digestion of walls from basaltic and basaltic-andesitic magma. Mostsamples are in the range of subalkaline to calc-alkaline series. Therefore, it can be concluded that even though the changing trends for main oxides of igneous rocks are somewhat linear and it actually shows magmatic differentiation in these rocks, factors such as alteration and magmatic contamination affected this trend. The presence of samples with clay minerals such as smectite, illite, and indicate that hydrothermal alteration in this region is acidic to neutral. While those samples with clay minerals of chlorite, calcite, and illite indicate that it is of neutral to alkaline type. Presence of chlorite, kaolinite, biotite, and epidote shows that formation temperature is higher than around 230°C. Further investigation is required for detail investigation of alteration mineralogy in the current well drilling progress.

6. ACKNOWLEDGMENT

First of all, I would like to thank Professor Ryuichi ITOI for his best advising service and to enable me get the well drill samples from the consultant company, WEST JEC. It is also my pleasure to thank WEST JEC and Mr. Matsuda. Professor Taguchi sensei, for his advising and follow up of our project study and field lecture in Hatchobarau and Otake geothermal field. I would like to thank Professor Thomas for his close assistance and advising in the Economic Geology Laboratory. Finally, I won`t forget all the Economic Geology Laboratory Ph.D., M.Sc. And B.Sc. students for their unlimited every day cooperation and assistance to give us a priorityto use the XRF, XRD equipment and the necessary laboratory instruments, and teach us how to operate, and during interpretation of the results.

7. REFERENCES

Abebe, T., Balestrieri, M.L. and Bigazzi,G.(2010) The Central Main Ethiopian Rift isyounger than 8 Ma:

Confirmation through apatite fission-track thermo chronology, Terra Nova, 22,6,470-476

Aoki, M., Comsti, E. C., Lazo, and Matsuhisa, Y. (1993). Advanced Argillic Alteration and Geochemistry of Alunite in an Evolving Hydrothermal System at Baguio, Northern Luzon Philippines. Resource Geol., 43, 155-164.

Boccaletti, M., Bonini, M., Mazzuoli, R., Trua, T.(1999) Pliocene-Quaternary volcanism and faulting in thenorthern Main Ethiopian Rift (with two geological maps at scale 1:50000). Acta Vulcanologica 11, 83–97.

Bonnini, M., Corti,G., Innocenti,F., Manetti,P., Mazzarini,F., Abebe,T. and Pecskay,Z.(2005) Evolution of the Main Ethiopian Rift in the frame of Afar, TECTONICS, 24, TC1007

Corti, G.(2008) Control of rift obliquity on the evolution and segmentation of the main Ethiopian rift. Nature Geoscience 1, 258–262.

Corti, G.(2009) Continental rift evolution: From rift initiation to incipient break-up in the Main Ethiopian Rift, East Africa, Earth-Science Reviews, 96, 1-53

Cox, K.G., Bell,J.D. and Pankhurst, R.J.(1979) The Interpretation of Igneous Rocks, Allen & Unwin, London, pp450

Davidson, A. and Rex, D.C.(1980) Age of volcanism and rifting in southwestern Ethiopia, Nature, 283, 657- 658.

Hayashi, M. (1973) Hydrothermal alteration in the Otake geothermal area, Kyushu, Chinetsu, 10(3), 9-46.

Hayashi, M.(2013), Geological Exploration of Geothermal Resources, Kyushu University 36, Hakozaki,Fukuoka 812, Japan.

Miyashiro, A.(1974) Volcanic rock series in island arcs and active continental margins. American Journal ofScience, 274, 321–355

Peccerillo, A. and Taylor, S.R.(1976) Geochemistry of Eocene Calc-Alkaline Volucanic Rocks from theKastamonu Area, Northern Turkey, Contributions to Mineralogy and Petrology, 58, 63-81

Reyes, A.G. (1990) Petrology of Philippine geothermal systems and the application of alteration mineralogy totheir assessment. J, Volcano. and Geotherm. Res., 43, 279-309.

Taguchi, S. (2001), Otake-Hatchobarau geothermal field: Society of Economic Geologist Guidebook 34, 173-177.

Taguchi, S., Oikawa, K., Kiyosaki, J., Chiba, H. and Motomura, Y. (2003) Manifestation of High TemperatureHypogene Acid Alteration in steaming Ground at the Hatchobarau Geothermal Field, Kyushu, Japan, Proceedings 25 NZ Geothermal Workshop 2003, 161-165.

Timothy E. La Tour (1989), Analysis of Rocks Using X-Ray Fluorescence Spectrometry, The Rigaku JournalVol. 6.